

# Archival Report

## The Functional Brain Organization of an Individual Allows Prediction of Measures of Social Abilities Transdiagnostically in Autism and Attention-Deficit/Hyperactivity Disorder

Evelyn M.R. Lake, Emily S. Finn, Stephanie M. Noble, Tamara Vanderwal, Xilin Shen, Monica D. Rosenberg, Marisa N. Spann, Marvin M. Chun, Dustin Scheinost, and R. Todd Constable

### ABSTRACT

**BACKGROUND:** Autism spectrum disorder and attention-deficit/hyperactivity disorder (ADHD) are associated with complex changes as revealed by functional magnetic resonance imaging. To date, neuroimaging-based models are not able to characterize individuals with sufficient sensitivity and specificity. Further, although evidence shows that ADHD traits occur in individuals with autism spectrum disorder, and autism spectrum disorder traits in individuals with ADHD, the neurofunctional basis of the overlap is undefined.

**METHODS:** Using individuals from the Autism Brain Imaging Data Exchange and ADHD-200, we apply a data-driven, subject-level approach, connectome-based predictive modeling, to resting-state functional magnetic resonance imaging data to identify brain-behavior associations that are predictive of symptom severity. We examine cross-diagnostic commonalities and differences.

**RESULTS:** Using leave-one-subject-out and split-half analyses, we define networks that predict Social Responsiveness Scale, Autism Diagnostic Observation Schedule, and ADHD Rating Scale scores and confirm that these networks generalize to novel subjects. Networks share minimal overlap of edges (<2%) but some common regions of high hubness (Brodmann areas 10, 11, and 21, cerebellum, and thalamus). Further, predicted Social Responsiveness Scale scores for individuals with ADHD are linked to ADHD symptoms, supporting the hypothesis that brain organization relevant to autism spectrum disorder severity shares a component associated with attention in ADHD. Predictive connections and high-hubness regions are found within a wide range of brain areas and across conventional networks.

**CONCLUSIONS:** An individual's functional connectivity profile contains information that supports dimensional, nonbinary classification in autism spectrum disorder and ADHD. Furthermore, we can determine disorder-specific and shared neurofunctional pathology using our method.

**Keywords:** ADHD, Autism spectrum disorder, Functional connectivity, Functional MRI, Magnetic resonance imaging, Predictive modeling

<https://doi.org/10.1016/j.biopsych.2019.02.019>

The assessment of autism spectrum disorder (ASD) is challenging, in part because ASD includes a spectrum of symptoms, skills, and levels of impairment (1). As such, diagnosis, severity estimates, and treatment choices often vary widely across individuals. Reflecting this clinical complexity, the associated neural correlates are also complex, have been difficult to characterize, and are not well understood (2). Similarly, attention-deficit/hyperactivity disorder (ADHD) is characterized by multisystem structural and functional brain abnormalities that present in varied ways within the population (3). Together, ASD (prevalence ~2%) and ADHD (~6%) are the most common childhood neurodevelopmental disorders

(4,5). Furthermore, across referred and nonreferred populations, symptoms of ASD occur with greater frequency (20%) in children with ADHD, and ADHD symptoms occur with greater frequency (30%–50%) in children with ASD (6–8). Yet, the underlying neurofunctional basis of the interplay between disorders is undefined and understudied (9,10).

Despite the overlap in clinical presentation, ASD and ADHD are defined as distinct disorders (11). As such, there are a limited number of studies that investigate these disorders together within the same work. Among those that do, there is a lack of consensus (10,12–14). Furthermore, there are controversial findings regarding genetic overlap between ASD and ADHD (15–17).

Functional magnetic resonance imaging is a noninvasive methodology that can measure a correlate of brain activity (18). The dynamic time-series functional magnetic resonance imaging data can be analyzed to identify patterns of coupling between distinct anatomical regions: a measure referred to as functional connectivity (FC) (19). A map of all the connections in the brain is referred to as the functional connectome (20). Recent work has demonstrated that individuals have unique FC patterns that contain information about behavioral traits or clinical symptoms, or both, which may prove useful in guiding individualized clinical management (12,21–25). Specifically, Finn *et al.* (21) demonstrates that FC can be used to predict fluid intelligence. Furthermore, others have demonstrated the utility of this method in predicting openness, attention, and intelligence (22–25).

FC studies of ASD show alterations in multiple functional networks compared with those of typically developing (TD) individuals (2,9,26–30). Similarly, altered FC has been documented in individuals with ADHD and transdiagnostically (9,30–33). However, studies demonstrating a continuous relationship between behavioral measures (gold-standard clinical evaluation) and FC are very limited, as the vast majority focus on diagnosis (26,34). Furthermore, few studies predict out-of-sample—rather than explain within-sample—clinical scores, many are underpowered, and the results are rarely replicated (3,26,34–36). As recent reviews summarize, findings in this area are generally complex and nonconverging, likely reflecting both the heterogeneity of these disorders and the disparate but relevant brain circuits investigated (37–39).

Given the substantial individual differences in ASD and ADHD symptomatology and the complex imaging correlates, a whole-brain data-driven dimensional approach focused on individual differences rather than categorical or binary grouping may be more useful in capturing features across multiple brain circuits. Here, we test the hypothesis that connectome-based predictive modeling (CPM) can be used to identify complex whole-brain networks that predict symptom severity (21,25,40). Notably, CPM networks can be difficult to interpret. Therefore, we implement two strategies to describe our results in more familiar framework: overlap of edges with a priori networks, and regions of high hubness (41,42).

We focus on two clinical scores relevant to ASD, the Social Responsiveness Scale (SRS) and the Autism Diagnostic Observation Schedule (ADOS), available from the Autism Brain Imaging Data Exchange (ABIDE) as well as the ADHD Rating Scale IV (ADHD-RS) available from the ADHD-200 (43–45). Using both leave-one-subject-out (LOO) and split-half cross-validation, we validate our models and define three functional networks related to SRS, ADOS, and ADHD-RS scores. We explore the generalizability of our models within and across disorders (6–8,17,46–48).

## METHODS AND MATERIALS

## Data Sets

We analyzed data from ABIDE-I/II and the ADHD-200 consortium, two publicly available multisite data sets of resting-state functional magnetic resonance imaging, demographic, and clinical assessment data (43–45). Details available for ABIDE-I/II at [fcon\\_1000.projects.nitrc.org/indi/abide/](http://fcon_1000.projects.nitrc.org/indi/abide/) and

ADHD-200 at fcon\_1000.projects.nitrc.org/indi/adhd200/. Refer to the [Supplement](#) for imaging parameters.

## Data Processing

Standard preprocessing was applied (see the [Supplement](#)) (23,49,50). For each individual, a  $268 \times 268$  connectivity matrix was calculated using a functional atlas defined on a separate population (21,41). Each entry in the matrix represents the strength of the functional connection between two nodes, also referred to as an “edge,” and the matrix as a whole is the individual’s functional connectome.

## Behavior Metrics

From ABIDE-I/II, we used SRS score, which serves as a broad-spectrum estimate of autistic traits across ASD and TD individuals (51). We also used a more intensive scale, ADOS, which is exclusive to ASD (52). From ADHD-200, we included the ADHD-RS IV (53). Refer to the [Supplement](#) for details and examples.

## Model Building: Behavior Prediction

Models were built using LOO cross-validation CPM (21,23,40). There are three steps: 1) feature selection ( $n - 1$  training set), 2) building of a predictive model ( $n - 1$  training set), and 3) testing the left-out subject. Each individual is left out once in an iterative framework, which builds a network of predictive edges and predicted scores for all individuals. Refer to [Supplemental Figure S2](#) for an illustrated description (54). Motion was not regressed during this analysis, and diagnosis did not enter into the model. No normalization of score (across module/version) was necessary, as only one was used to build each model ([Supplemental Table S1](#)). Finally, while partial correlation-based FC measures have been validated, here there are fewer observations (i.e., frames or time points) than nodes (55–57). Therefore, to avoid the pitfalls of arbitrary parameterization, we chose not to do partial correlation. We applied Bonferroni correction for multiple comparisons (six SRS, four ADOS, and three ADHD-RS scores).

## Internal Validation: Split-Half Cross-Validation, Permutation Testing, and Extrapolation

To test model robustness, we used split-half validation ( $n = 200$  iterations) and permutation testing ( $n = 1000$  iterations). For split-half validation, individuals were divided equally between train and test groups by random selection. Network on model building was conducted within the training group as described above, and the model was applied to the test group. For permutation testing, subject labels and clinical scores were randomly shuffled to break the true brain-behavior relationship, and then prediction was performed on the shuffled data to generate a null result (40). We tested whether correlations from train and/or test and shuffled data come from different distributions (Kruskal-Wallis; MATLAB; The MathWorks, Inc., Natick, MA). Within each split-half iteration, networks and models were applied (extrapolated) to all individuals (less those used to generate the model) whether or not clinical scores were available from these individuals. Thus, for each individual, we generated an average clinical score prediction that we compared between diagnosis groups (anova1, MATLAB). We

applied Bonferroni correction for multiple comparisons. To avoid “double-dipping,” scores were never predicted for individuals who were within the network- or model-building group.

### Network Anatomy of Edges

The brain is complex, and the networks identified by CPM reflect this complexity. To assess the extent to which our models share common features, we computed the probability that  $n$  shared edges exist between our networks and edges within or between 10 atlas networks (41,42). Significance was determined using the hypergeometric cumulative distribution function (hygecdf, MATLAB, Bonferroni correction for 55 comparisons). We report the likelihood ( $1.0 - p$  value) that each atlas network (and internetwork pair) contributed to our networks.

Furthermore, we analyzed the distribution of edge lengths within our networks (defined as the Euclidean distance between the center of mass between nodes). Using MATLAB, we tested for outliers (kurtosis), normalcy (lillietest), a tendency toward long or short connections (skewness), and differences between positive/negative network distributions (ranksum). In addition, we evaluated the anatomy of shared features between networks by taking the products of positive/positive, positive/negative, negative/positive, and negative/negative network pairs across scales and computed the likelihood that each of the resulting sets of shared features contains  $n$  edges.

### Node Hubness

Above, we described overlap using shared edges. Here, we identify nodes within our networks with high hubness (i.e., with a greater number of connections to other nodes). We calculated hubness by taking the node with the greatest number of edges (connections to other nodes) within a network and dividing the number of edges connecting to each node within the given network by this maximum value. Thus, for each node in a network, we obtained a number (0–1) that scales relative to the greatest number of connections (or highest hubness). Although this allows inferences to be made about the most connected nodes within our networks, it should be emphasized that CPM is driven by edges, not nodes.

## RESULTS

Results generated from ABIDE-I/II data precede results generated from ADHD-200 data followed by the cross-diagnosis comparison.

### Participants

Exclusion criteria are described in the Supplement (58). To account for site effects, we repeat our analysis in a leave-one-site-out framework (Supplemental Figure S3). We observe no change in our findings. However, it should be noted that this is an imperfect method, and site effects could still be influencing our observations. On the other hand, a study such as this is impossible without the participation of multiple sites.

### ASD Behavior Prediction (ABIDE-I/II)

For all SRS subscales, predicted behavior correlated with known scores ( $r = .23\text{--}.37$ ,  $p < .00002$ ) (Figure 1A). Similar

results were obtained for ADOS scores ( $r = .43\text{--}.60$ ,  $p < .0002$ ) (Figure 1B). In all cases, age, Full IQ Standard Score (FIQ) and motion were included along with our model as covariates (Supplemental Table S1). As a secondary analysis, we considered only male individuals and obtained comparable results (Supplemental Table S1C, D). Insufficient data were available for a female group. These results affirm our hypothesis that CPM can be used to predict the severity of ASD symptoms. That is, the individual’s functional connectome contains information reflecting social behavioral scores as measured by SRS and ADOS.

### Internal Validation of SRS and ADOS Models

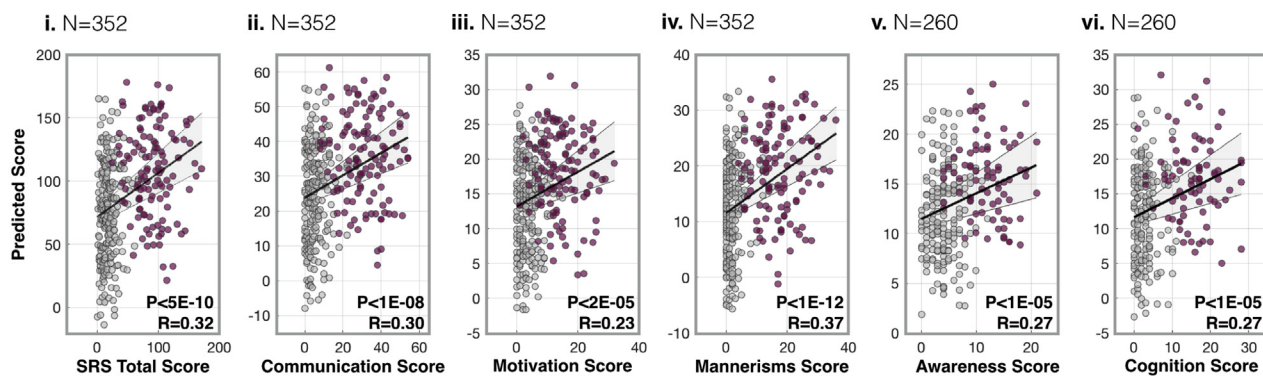
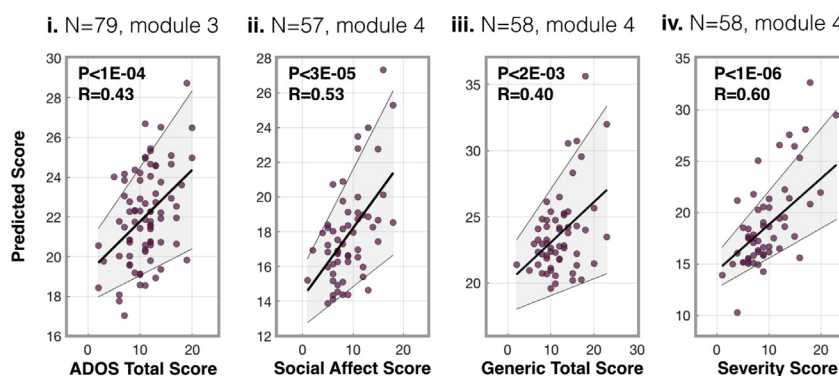
To test the robustness of our models and generalizability within ABIDE-I/II, we used split-half cross-validation and permutation testing. Correlations between known and predicted behavior for split-half train and test groups are plotted alongside correlations obtained from shuffled data (null results) (Figure 2A). For all SRS and ADOS subscales, correlations from train and test data were greater than those from shuffled data. When SRS and ADOS models were applied to all individuals (less those used to generate the model), mean predicted scores (across iterations) were greater for individuals with ASD relative to TD individuals ( $N = 632$ ) (Figure 2B), with the exception of the ADOS Severity subscale. As a control, whole-brain connectivity in place of SRS and ADOS networks showed no difference between diagnostic groups (Supplemental Figures S5 and S6C). Note that networks and models generated within this section are not used in future sections. Networks from the section ASD Behavior Prediction (ABIDE-I/II) (generated from all individuals) are applied in all following analyses.

### Anatomy of SRS/ADOS Networks

Unsurprisingly, given that subscale scores are highly correlated (Supplemental Figure S1A), the anatomy of subscale networks are similar (e.g., across SRS subscales, positive edges are very likely to overlap with edges within the cerebellum). On the other hand, there are notable exceptions where subscale network anatomy diverges (e.g., edges between medial-frontal and motor networks were very likely to occur within SRS total, communication, motivation, and mannerism positive subscale networks, but unlikely to occur within SRS cognition and awareness positive subscale networks) (Figure 3, examples highlighted). Although it is difficult to summarize the complex networks generated with CPM, here feature sets that contribute most to SRS and ADOS networks are described in a more familiar framework.

### Composite SRS and ADOS Networks

As a data reduction strategy before investigating model generalizability, and to identify edges that contribute across subscales, “low” to “high” threshold, “composite” networks are defined as follows: lowest, edges that appear in any subscale network at least once; highest, edges that appear in all subscale networks. Note that this is a threshold applied not at the feature selection step but at the level of comparing networks for cross subscale relevance. The anatomy of composite networks across thresholds is summarized in Supplemental Figure S7. Despite similar anatomy at the

**A** CPM results for SRS sub-scales (+ve) + (-ve): □ TD ■ ASD**B** CPM results for ADOS sub-scales (+ve) + (-ve): ■ ASD

**Figure 1.** Leave-one-subject-out cross-validation connectome-based predictive modeling (CPM) results for Social Responsiveness Scale (SRS) and Autism Diagnostic Observation Schedule (ADOS) subscale scores. **(A)** Leave-one-subject-out cross-validation CPM results for SRS subscale scores. For each SRS subscale (i–vi), the sums of the predicted SRS score from positive and negative models are plotted against known scores. **(B)** Leave-one-subject-out cross-validation CPM results for ADOS subscale scores. For each subscale (i–iv), the sums of the predicted ADOS score from positive and negative models are plotted against known scores. The linear regression is shown in black, and the 95% confidence interval is shown in gray. –ve, negative; +ve, positive; ASD, autism spectrum disorder; TD, typically developing.

network level between subscale networks, at the edge level, there was an order of magnitude difference in the number of edges contained within composite networks at the lowest versus highest threshold (*Supplemental Figure S7*).

The anatomy and distribution of edge lengths (see the section Edge Lengths [ASD]) in composite networks were similar across thresholds. The feature that distinguished edges in the low-threshold networks from those in the high-threshold networks was the magnitude of the slope in the linear model relating edge strength to clinical score. Yet composite network predictive power changed little with threshold, which is notable considering the difference in the number of edges between thresholds (*Supplemental Figure S8C*). For all between-scale comparisons (see the sections Model Generalizability [ADOS vs. SRS] and Model Generalizability [SRS and ADOS Models in ADHD]), composite networks were formed with edges that appeared in three or more subscale networks.

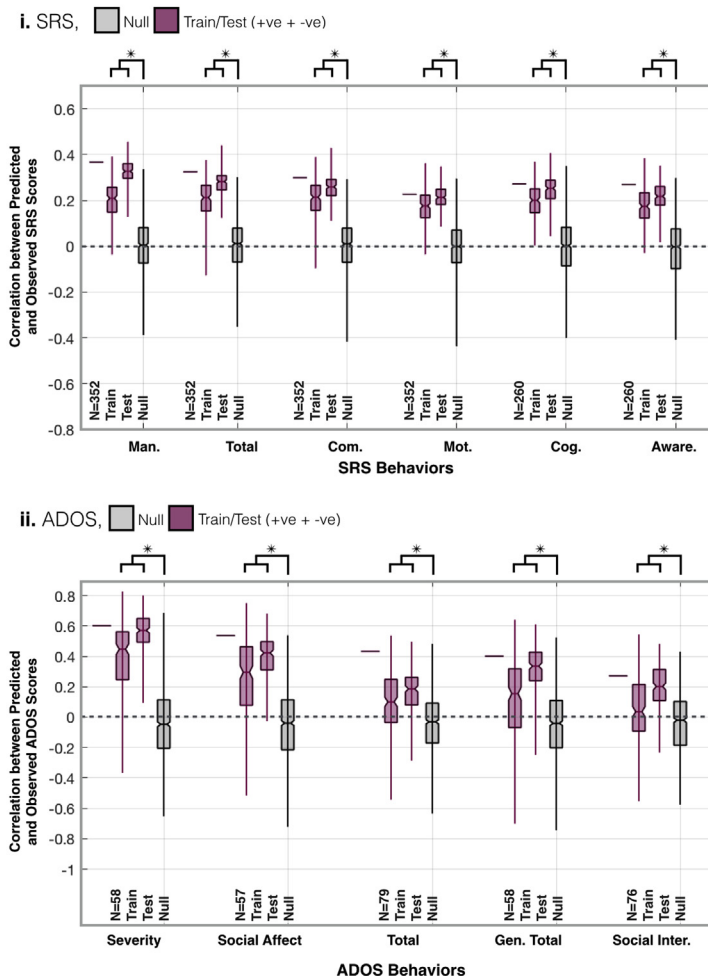
### Edge Lengths (ASD)

Motivated by controversy in the literature regarding long- and short-range hyper- and hypoconnectivity in ASD, we analyzed

the distribution of edge lengths in positive/negative subscale and composite networks (*Supplemental Figure S8A, B*). None of our networks contain outliers. For networks that were not normally distributed, edges skewed toward longer lengths. For subscale and composite SRS networks, there was no difference in median edge length between positive and negative networks. On the other hand, although the difference was small (~0.5 cm), negative edges were longer than positive edges in most subscale and composite ADOS networks. In summary, we find weak evidence of longer edges contributing more to symptom severity in ASD.

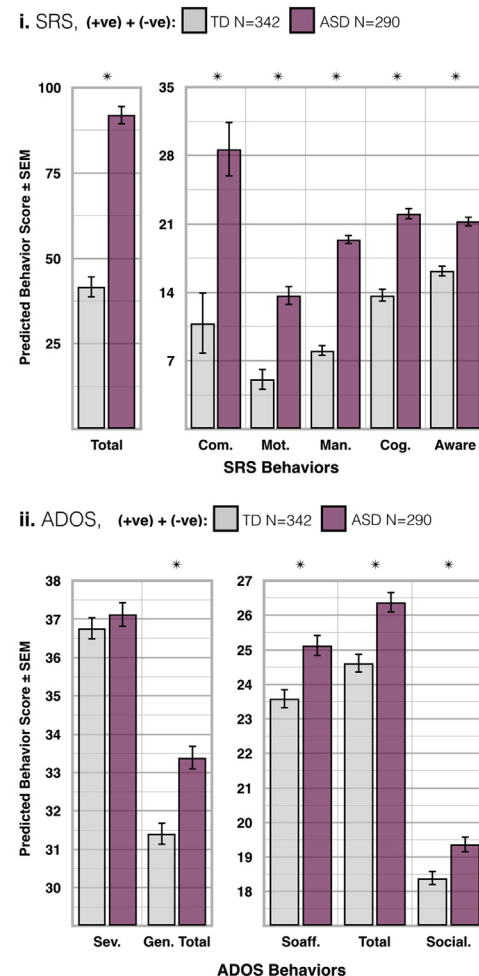
### Model Generalizability (ADOS vs. SRS)

Model generalizability was tested within ABIDE-I/II, and across data sets and diagnoses (see the section Model Generalizability [SRS and ADOS Models in ADHD] and *Figure 4*). Within ABIDE-I/II, SRS composite networks were applied to individuals from ABIDE-I/II for whom ADOS, but not SRS, scores were available. Likewise, ADOS composite networks were applied to individuals with SRS but without ADOS scores. Predicted SRS scores correlated with known ADOS social

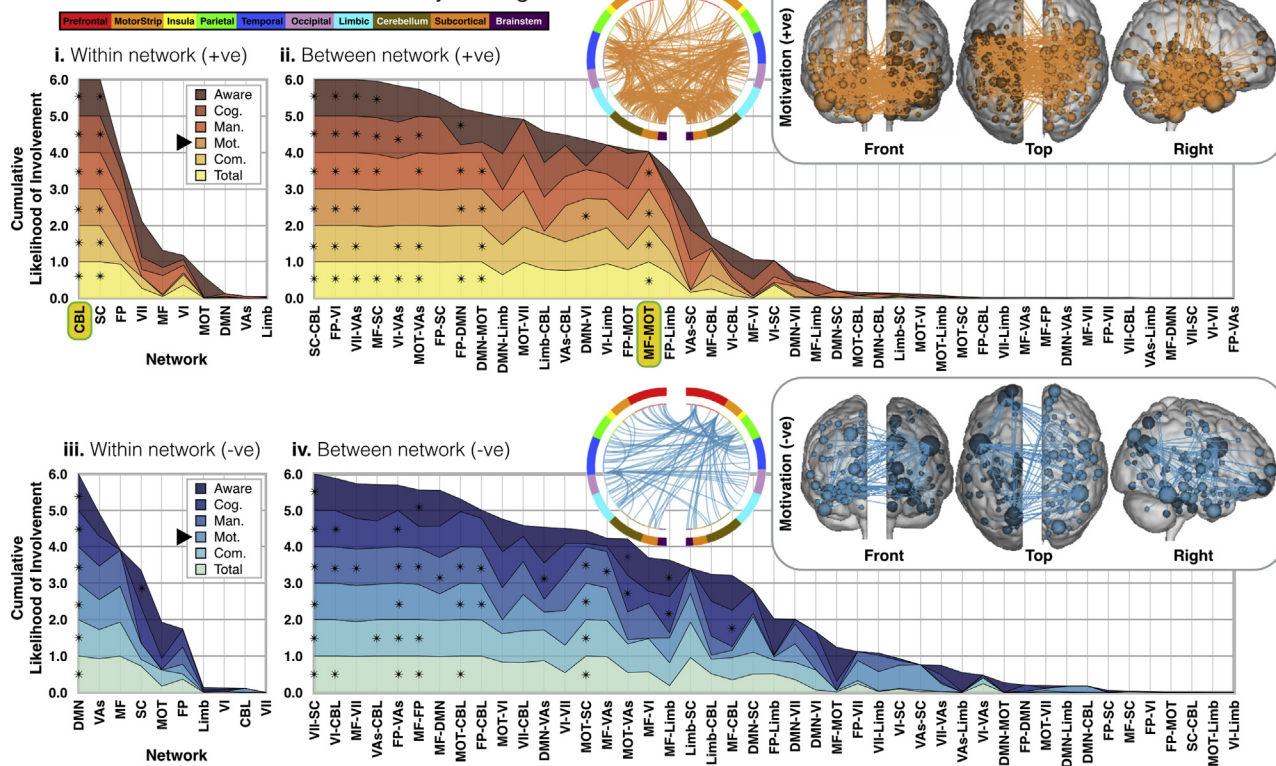
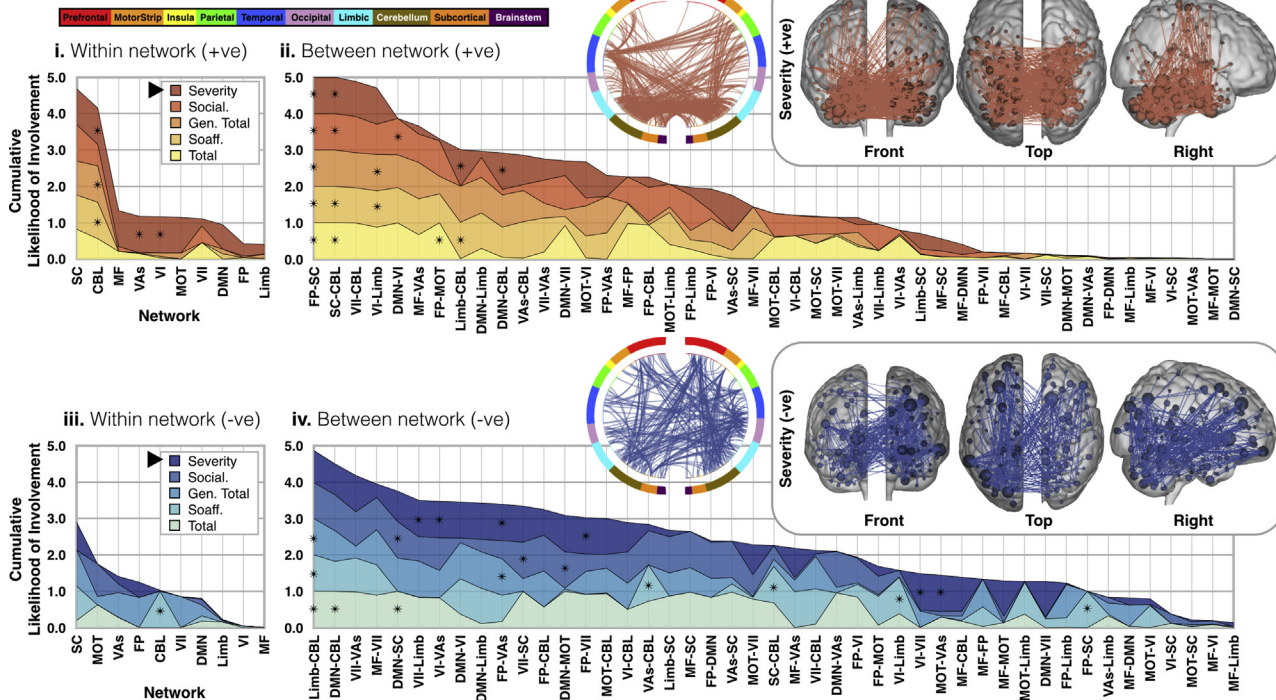
**A** Split-half cross-validation and permutation testing

**Figure 2.** Social Responsiveness Scale (SRS) and Autism Diagnostic Observation Schedule (ADOS) split-half cross-validation and permutation testing results and application to all individuals from the Autism Brain Imaging Data Exchange I and II sets. **(A)** Correlation ( $r$  value) for split-half cross-validation. (i) For each SRS subscale, the bar in the leftmost column is reproduced for reference from the leave-one-subject-out cross-validation connectome-based predictive modeling (CPM) results reported in Figure 1.  $n = 352$  for the total, mannerisms, communication, and motivation scores,  $n = 260$  for the cognition and awareness scores. The middle two columns are from split-half train and test cross-validation CPMs ( $n = 200$  iterations). The final column shows the null results from permutation testing where participants and scores are scrambled prior to leave-one-subject-out cross-validation ( $n = 1000$ ). For all SRS subscales, train and test results are greater than null results ( $p < 2 \times 10^{-144}$ ). (ii) For each ADOS subscale ( $p < .03$ ), the bar in the leftmost column is reproduced for reference from the leave-one-subject-out cross-validation CPM results reported in Figure 1. The middle two columns are from split-half train and test cross-validation CPMs ( $n = 200$  iterations). The final column shows the null results from permutation testing where participants and scores are scrambled prior to leave-one-subject-out cross-validation ( $n = 1000$ ). See Supplemental Figures S3A and S4A for results from SRS and ADOS positive and negative feature sets. **(B)** From each iteration of the split-half cross-validation, the model was applied to all individuals from the Autism Brain Imaging Data Exchange I and II groups less those in the training group ( $n = 632$  training) to predict clinical scores. Across iterations ( $n = 200$ ), mean predicted scores are compared between typically developing (TD) individuals and individuals with autism spectrum disorder (ASD). (i) For all subscales, predicted SRS scores ( $p < 1 \times 10^{-7}$ ) are greater for individuals with ASD than for TD individuals. (ii) Likewise, all but the severity ADOS subscale score was greater for individuals with ASD than for TD individuals ( $p < .02$ ). Between ASD and TD groups, motion ( $p > .14$ ) and age ( $p > .96$ ) were not different. -ve, negative; +ve, positive; Aware., Awareness subscale score; Cog., Cognition subscale score; Com., Communication subscale score; Gen. Total, Generic Total score; Man., Mannerism subscale; Mot., Motivation subscale score; Sev., Severity score; Soaff., Social Affect subscale score; Social Inter. or Social, Social Interaction subscale score.

affect ( $r = .36, p < .01$ ) and generic total ( $r = .29, p < .03$ ) scores. Likewise, predicted ADOS scores correlated with known SRS mannerisms ( $r = .16, p < .01$ ) and cognition scores ( $r = .20, p < .002$ ) (Figure 5A). Note that the predicted scores here are not true SRS or ADOS scores, as they are generated using composite networks.

**B** CPMs applied to all individuals, N=632**Model Generalizability (SRS and ADOS Models in ADHD)**

Motivated by the idea that the underlying biology of mental health disorders is not merely categorical, but rather trans-diagnostic, we tested network specificity by applying our SRS and ADOS models to children with ADHD and our ADHD model

**A** SRS - Functional network identity of edges**B** ADOS - Functional network identity of edges

**Figure 3.** Anatomy of Social Responsiveness Scale (SRS) and Autism Diagnostic Observation Schedule (ADOS) subscale networks. For (A) SRS and (B) ADOS, edge overlap (i, iii) within and (ii, iv) between 10 a priori atlas networks and our connectome-based predictive modeling networks are plotted for (i, ii) positive and (iii, iv) negative feature sets. Each layered plot shows the cumulative (sum) likelihood ( $1.0 - p$  value) estimated from the probability of edges being shared between a priori networks and each SRS and/or ADOS subscale network. Notice that in all plots, networks and internetwork pairs are ordered from greatest to least cumulative likelihood (i.e., the x-axis is ordered differently in each plot). Overall, the subscale networks appear similar (e.g., highlighted in A).

to children with ASD (32,47,59,60). To facilitate this comparison, we first implemented the same procedures described above for ABIDE-I/II data, to predict ADHD symptoms within the ADHD-200 data set (Figure 4A). Correlations between known and predicted scores were found to be significant using split-half cross-validation and permutation testing (Figure 4B). As above, we also examined the anatomy of ADHD subscale (Figure 4C, D) and composite (Supplemental Figure S9) networks.

Across neurodevelopmental disorders, predicted SRS scores correlated with known ADHD scores ( $r = .31$  or  $.32$ ,  $p < .01$ ) (Figure 5B). This result indicates that the SRS model contains components related to attention that account for significant variance in predicting ADHD symptoms. However, in each cross-index model test (present and previous section), predictive power was worse than that of the model constructed with the score of interest (e.g., predicted inattention for individuals with ADHD [Figure 4A],  $r = .40$ , is a stronger relationship than predicted “SRS” score from applying the composite SRS network to individuals with ADHD [Figure 5B],  $r = .32$ ).

### Shared Anatomy of Composite Networks Across Scales at the Edge and Network Levels

To investigate whether predictions across scales were a by-product of common anatomy, shared features were quantified at the edge, network, and regional levels. The anatomy of shared edges was estimated by taking the products of composite network pairs and computing the likelihood ( $1.0 - p$  value) that each of the resulting sets of shared features contains  $n$  edges from atlas networks. These results are summarized in  $2 \times 2$  matrices of layer plots for all thresholds (Figure 5C, D). Shared network-level features were summarized and compared with shared edge-level features (Supplemental Figure S10). For each composite network, the contributing atlas networks and atlas-network pairs are listed. Common atlas-network features are indicated between composite networks, as are features implicated at the edge level. The cerebellum contributes to SRS and ADOS (positive), frontal-parietal to visual areas contribute to SRS and ADOS (negative), subcortical and frontal-parietal to visual-I contributes to SRS and ADHD (positive), and default mode contributes to SRS and ADHD (negative). However, only SRS and ADHD (negative) share edges that contribute significantly to both networks.

### Regions of High Hubness ASD and ADHD

Above, networks are described in terms of overlapping edges contained within and between 10 a priori atlas networks. Here, nodes with high hubness (i.e., with a greater number of connections to other nodes) are identified to further characterize ASD and ADHD networks. Supplemental Figures S11–S13 show surface maps of SRS, ADOS, and ADHD networks using hubness to illustrate nodes that play a greater role in the brain-behavior relationships we observe. Nodes with high hubness ( $>0.5$ ) span a wide range of brain functions. At this

moderate threshold, several regions are shared between ASD and ADHD (Supplemental Tables S2 and S3). However, as described above, edges do not overlap between ASD and ADHD networks. Thus, although many of the same regions are implicated when we use hubness to describe our findings, this is perhaps misleading because it is the connections between regions that drive the brain-behavior relationships observed here.

### Replication Without Global Signal Regression

LOO CPM and split-half cross-validation on ABIDE-I/II and ADHD-200 data without global signal regression was performed (Supplemental Table S4 and Supplemental Figure S14). Overall, our findings are unchanged, although stronger results are obtained when global signal regression is applied.

## DISCUSSION

Using open-source data and a novel prediction framework, we find meaningful FC patterns that can independently predict clinical measures of ASD and ADHD symptom severity (48). Specifically, we build models that link brain and behavior, by identifying patterns of activity associated with clinical scores as well as crossover between scores (ADOS and SRS) and disorders (ASD and ADHD). We find that SRS, ADOS, and the ADHD-RS implicate different brain circuitry (share minimal edge overlap), yet there are components that are predictive of severity that translate across scales and/or disorders. The power of CPM is validated by predicting clinical scores of unseen individuals. Our models provide insight into the complex brain organization associated with ASD and ADHD, and the diffuse nature of the identified circuits helps to explain the historical difficulty of characterizing these disorders with more spatially limited approaches. The network metrics we identify map behavioral differences onto brain circuitry. Thus, the present work does not replace or replicate the utility of these tests but instead provides a link between behavioral differences and brain FC differences.

Our results are consistent with a growing body of literature suggesting that ASD and ADHD contain partially overlapping but independent comorbidities (32,47,59,60). Notably, this relationship is not a by-product of high edge overlap:  $<2\%$  of edges are shared between any network pair. In line with previous results, our predictive networks are complex and widely distributed. Thus, they are not easily described. Nevertheless, we summarize our findings using a priori functional networks and high-hubness regions. We observe networks that have been implicated in the ASD literature: default mode, limbic, visuospatial, motor, subcortical, and cerebellum regions, and ADHD literature: cerebellum, subcortical to frontal-parietal, subcortical, default mode, medial-frontal, medial-frontal to limbic, motor, and visual areas (2,27–29,61,62). With our approach, we cannot conclude that one or a few networks “cause” ASD and/or ADHD symptoms. Rather, we observe a convergence of

However, there are exceptions where the anatomy diverges (e.g., highlighted in Aii). Insets show the edges of example SRS and ADOS positive and negative subscale networks as circle plots as well as edges or nodes overlaid on glass brains. \*Likelihood greater than chance. –ve, negative; +ve, positive; Aware., Awareness subscale score; CBL, cerebellum; Cog., Cognition subscale score; Com., Communication subscale score; DMN, default mode network; FP, frontoparietal lobe; Gen. Total, Generic Total score; Limb, limbic system; Man., Mannerism subscale; MF, mediofrontal cortex; MOT, motor areas; Mot., Motivation subscale score; SC, subcortical areas; Soaff., Social Affect subscale score; VAs, visual areas; VI, visual-I; VII, visual-II.

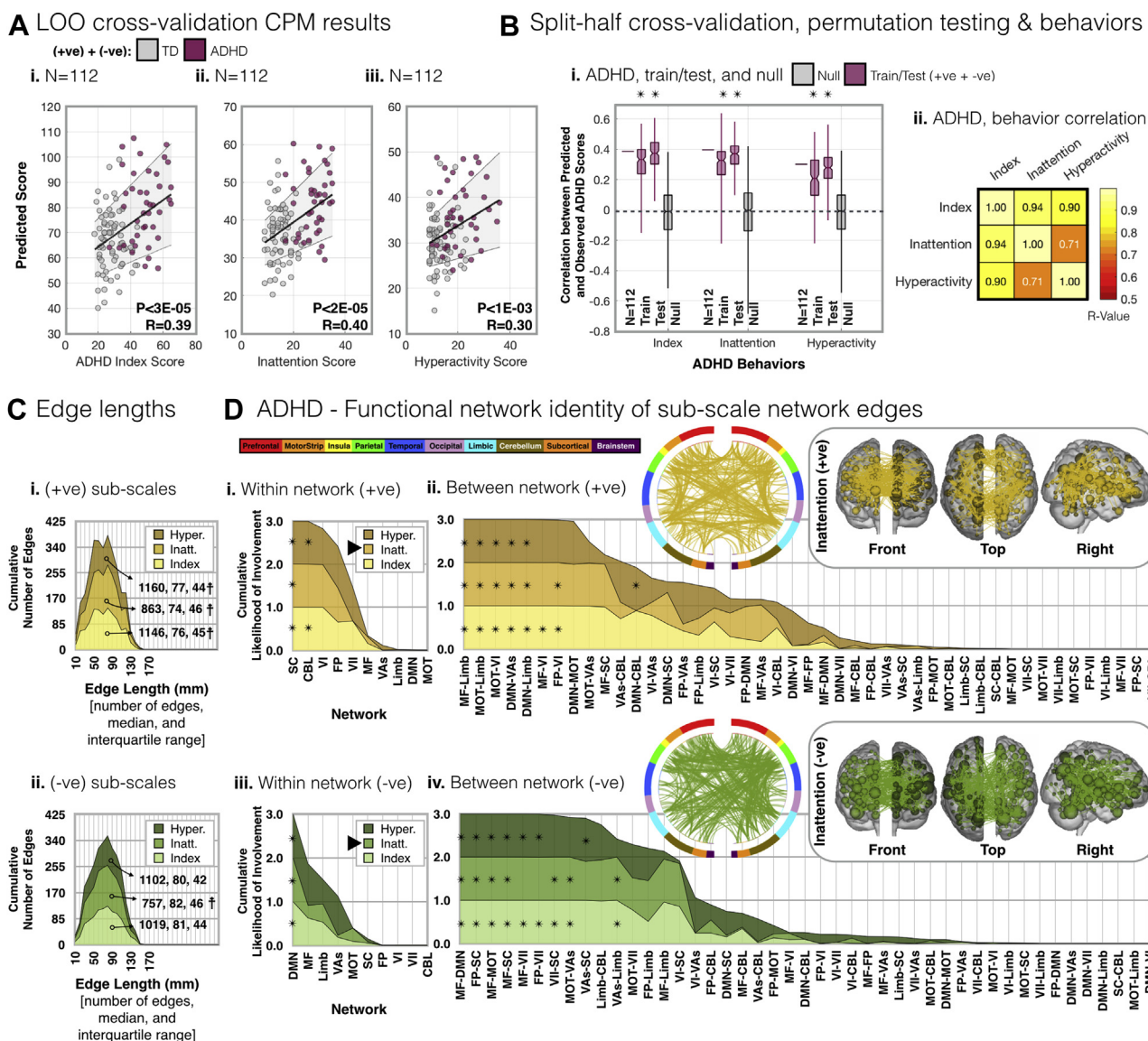


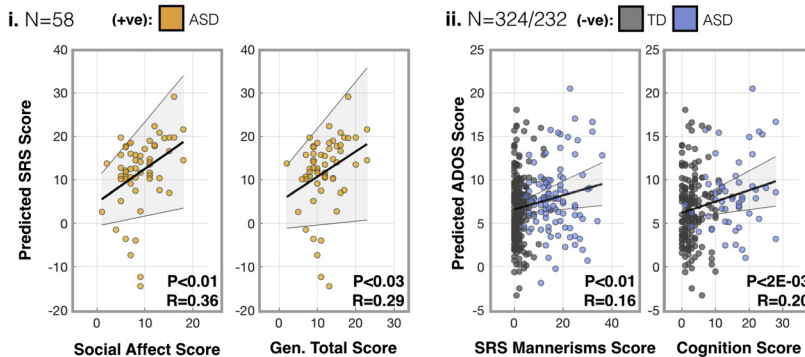
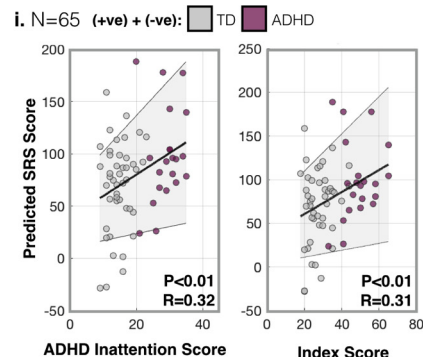
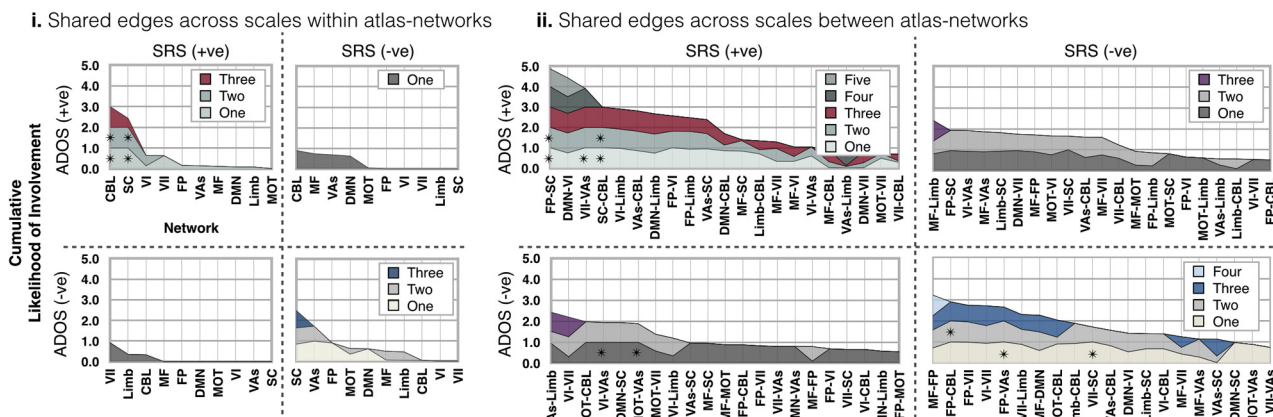
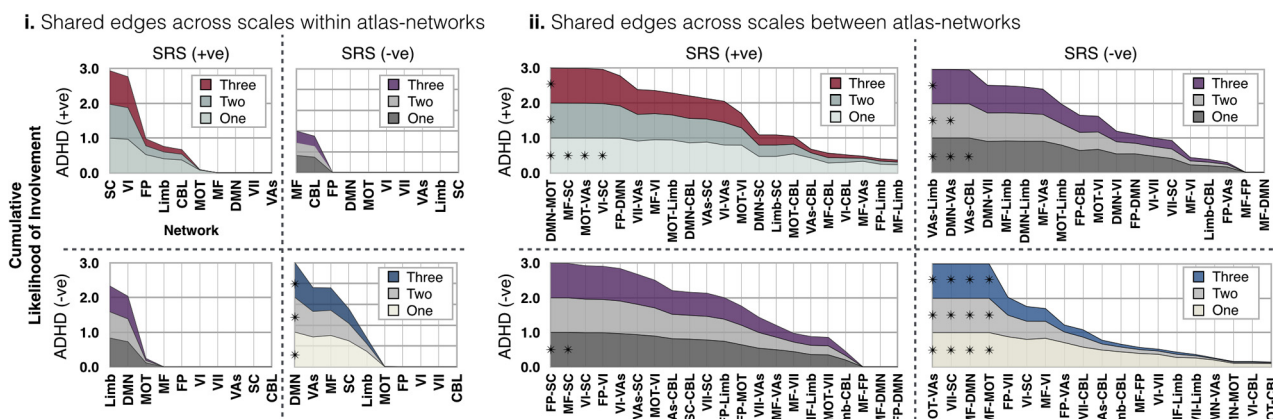
**Figure 4.** Results from individuals with attention-deficit/hyperactivity disorder (ADHD) and typically developing (TD) individuals from the ADHD-200 data set. As in **Figure 1A and B**, panel (A) gives leave-one-subject-out (LOO) cross-validation connectome-based predictive modeling (CPM) results for ADHD subscale scores. For each subscale (i–iii) the sum of the predicted ADHD score from the positive and negative models are plotted against known score. (B) As in **Figure 2A**, panel (i) gives the correlation ( $r$  value) of split-half cross-validation CPMs ( $n = 200$ ) for each ADHD subscale and null results from shuffled data ( $n = 1000$ ). As in **Supplemental Figure S1A**, panel (ii) gives the correlation matrix of ADHD behavior subscale scores. As with Social Responsiveness Scale and Autism Diagnostic Observation Schedule, ADHD subscale scores are highly correlated. As in **Supplemental Figure S7A** panel (i) and B panel (i), panel (C) shows layer plots of the cumulative number of edges vs. edge length for ADHD subscale networks. For all networks that are not normally distributed, edges are skewed toward longer lengths. None of the networks are prone to outliers. There is a difference between positive and negative feature set edge lengths for all subscale networks ( $p < 4 \times 10^{-3}$ ). As in **Figure 3**, panel (D) shows ADHD edge overlap (i, iii) within and (ii, iv) between 10 a priori atlas networks and ADHD networks are plotted for (i, ii) positive and (iii, iv) negative feature sets. Insets show the edges of example subscale networks as circle plots as well as edges and/or nodes overlaid on glass brains. \*Likelihood greater than chance. †Network with edge lengths that are not normally distributed. CBL, cerebellum; DMN, default mode network; FP, frontoparietal lobe; Limb, limbic system; MF, mediofrontal cortex; MOT, motor areas; SC, subcortical areas; VAs, visual areas; VI, visual-I; VII, visual-II.

functional connections that relate to a spectrum of behaviors. We assert that this is indeed a strength of the CPM approach that affords the ability to resolve more nuanced information by requiring fewer statistical tests. Furthermore, our methodology is designed to model the underlying biology of mental health disorders as a continuous spectrum, not merely as a

categorical definition. Such models can also be transdiagnostic, as we have demonstrated (63).

Overall, few high-hubness regions are shared between positive and negative ASD and ADHD networks. Within positive networks, both the thalamus and cerebellum have high hubness, indicating shared alterations in movement and

## Connectomics Characterization of Spectrum Disorders

**A** SRS/ADOS prediction of ADOS/SRS behavior scores**B** SRS prediction of ADHD scores**C** Shared edges between SRS and ADOS composite networks**D** Shared edges between SRS and ADHD composite networks

**Figure 5.** Generalizability of composite networks and overlap of composite network edges: Social Responsiveness Scale (SRS) and Autism Diagnostic Observation Schedule (ADOS) (positive and negative) and SRS and attention-deficit/hyperactivity disorder (ADHD) (positive and negative). Plotted in panels (A) and (B) are correlations of predicted vs. known behavior using composite networks applied across scales. We chose to threshold all composite networks at edges appearing in three or more subscale networks. In panel (A), the (i) SRS and (ii) ADOS composite networks were used to predict scores for individuals from Autism Brain Imaging Data Exchange I and II data sets for whom only the other score was available (i.e., the SRS network was used to predict scores for individuals for whom ADOS scores (not SRS scores) were available). Composite networks were also applied across the Autism Brain Imaging Data Exchange I and II and ADHD-200 data sets. (B) Predicted SRS scores correlate with known ADHD scores in individuals from the ADHD-200 data set. Layer plots showing the shared anatomy of (C) SRS and ADOS and (D) SRS and ADHD composite networks across thresholds. Composite network overlap of positive and negative feature sets was computed by taking the products—ADHD positive/SRS positive (upper left panel), ADHD positive/SRS negative (upper right panel), ADHD negative/SRS positive (lower left panel), and ADHD negative/SRS negative (lower right panel)—of paired networks and computing

sensation. Similarly, within negative networks, Brodmann areas (BAs) 10, BA 11, and BA 21 show high hubness, indicating common connectivity changes associated with changes in executive function and processing of language and/or semantics. On the other hand, if we consider high hubness collapsing across positive/negative networks and compare ASD (SRS and ADOS) versus ADHD, we observe more widespread patterns of connectivity alterations.

Specifically, transdiagnostically, we identify areas integral to executive function (BA 9, BA 10, BA 11, and BA 46) and vision (BA 7, BA 19, and primary and association vision areas). Likewise, we find representation/recognition (BA 31, BA 40, and insula) and language and/or semantics (BA 21, BA 22, BA 44, BA 47, primary auditory area, and cerebellum) areas that are shared between disorders. However, for this latter pair, we find additional areas within ASD networks (fusiform, BA 20, BA 39, and BA 45) that could indicate more ASD-specific dysfunction. Similarly, areas important for sensation (BA 40 and thalamus) and movement (BA 6, BA 7, BA 8, cerebellum, and thalamus) are found in ASD and ADHD. In ADHD, we identify additional areas (primary/association sensory areas, and primary motor areas). Finally, areas important for emotion (BA 24, BA 31, and BA 38, the hippocampus and insula), processing (BA 19, BA 21, BA 32, BA 47, and visual association areas), and memory (BA 38, parahippocampus, and hippocampus) are identified in both networks. Furthermore, across the same three dimensions, we identify additional areas unique to ASD—emotion (amygdala), processing (BA 39 and caudate), and memory (caudate)—and areas unique to ADHD—emotion (BA 23 and BA 25), processing (BA 25 and sensory association areas), and memory (BA 30). In summary, we find that ASD and ADHD share areas that are integral to a broad range of brain functions. This is not surprising given the heterogeneity and complexity of these disorders as well as the overall complexity of the human brain. Furthermore, our findings echo and extend previous work (9,10,12–14); see the *Supplement*.

Our results should be viewed in light of a few limitations, one of which is our strict inclusion criteria. On one hand, we include individuals on medication and individuals of both sexes in an attempt to reflect the true patient population and because we determined that clinical scores are independent of medication status and sex. Conversely, because age, FIQ, and motion are significantly correlated with clinical scores, we chose to limit these attributes to uncover connectivity features that relate only to clinical measures. Furthermore, to ensure that the features we identify are indeed specific to our metrics of interest, we built a model to predict FIQ, using the same data. We find that the underlying predictive features of the FIQ model are nonoverlapping with the features that are predictive of SRS and ADOS scores. Importantly, this indicates that the features within the SRS and ADOS models are specific to these measures.

Another consideration is the inherent heterogeneity of publicly available data, which likely made prediction more challenging. That we find CPM works despite this challenge should be considered a strength that may have improved

generalizability (64). Our models capture ~10% to 45% of the variance, which is in part due to the aforementioned heterogeneity. However, as we are building predictive (not explanatory) models and pooling from a large representative population, we expected modest effect sizes that are more generalizable (35,65). Finally, it should be noted that the correlative relationships between the functional connectome and clinical scores revealed by CPM cannot be used to infer causality.

Future studies could be improved by implementing longer imaging times and harmonized scanners and protocols, to provide more reliable FC measurements (42,66). It has also been suggested that data obtained while participants perform a task aimed at enhancing differences in connectivity can lead to better predictive models (67,68). Furthermore, the use of naturalistic conditions such as movie-watching can reduce motion, enhance individual differences, and improve an individual's tolerance of longer scan durations (69,70).

In conclusion, the present work uses a data-driven approach to develop objective quantitative models that establish a link between FC and behavior in ASD and ADHD. We observe widespread differences in functional organization, congruent with the complex behavioral and cognitive abnormalities that are a hallmark of these disorders. We also demonstrate the generalizability and transdiagnostic utility of this approach. In the future, understanding the changes in functional organization of the brain that relate to various dimensional aspects of behavior may provide the needed inferential leverage at the individual level to inform more comprehensive treatment strategies for individual patients and their families.

## ACKNOWLEDGMENTS AND DISCLOSURES

For ABIDE-I, primary support for the work by Adriana Di Martino was provided by the National Institute of Mental Health (Grant No. K23MH087770) and the Leon Levy Foundation. Primary support for the work by Michael P. Milham and the International Neuroimaging Data-sharing Initiative team was provided by gifts from Joseph P. Healy and the Stavros Niarchos Foundation to the Child Mind Institute, as well as by the National Institute of Mental Health (Grant No. R03MH096321 [to Michael P. Milham]). For ABIDE-II, primary support for the work by Adriana Di Martino and her team was provided by the National Institute of Mental Health (Grant No. 5R21MH107045). Primary support for the work by Michael P. Milham and his team was provided by the National Institute of Mental Health (Grant No. 5R21MH107045) and the Nathan S. Kline Institute of Psychiatric Research. Additional support was provided by gifts from Joseph P. Healey, Phyllis Green, and Randolph Cowen to the Child Mind Institute. The ADHD-200 work was coordinated by Michael P. Milham. Data collection at Peking University was supported by the following funding sources: the Commonwealth Sciences Foundation, Ministry of Health, China (Grant No. 200802073); the National Foundation, Ministry of Science and Technology, China (Grant No. 2007BAI17B03); the National Natural Sciences Foundation, China (Grant No. 30970802); the Funds for International Cooperation of the National Natural Science Foundation of China (Grant No. 81020108022); the National Natural Science Foundation of China (Grant No. 8100059); and the Open Research Fund of the State Key Laboratory of Cognitive Neuroscience and Learning.

A version of some material presented here appears on bioRxiv (bioRxiv 290320; doi: <https://doi.org/10.1101/290320>).

the likelihood that each atlas network contributes the observed number of edges to each set of shared features. \*Likelihood greater than chance. –ve, negative; +ve, positive; ASD, autism spectrum disorder; CBL, cerebellum; DMN, default mode network; FP, frontoparietal lobe; Gen. Total, Generic Total score; Limb, limbic system; MF, mediofrontal cortex; MOT, motor areas; SC, subcortical areas; TD, typically developing; VAs, visual areas; VI, visual; VII, visual-II.

The authors report no biomedical financial interests or potential conflicts of interest.

## ARTICLE INFORMATION

From the Department of Radiology and Biomedical Imaging (EMRL, XS, DS, RTC), Interdepartmental Neuroscience Program (SMN, MMC, RTC), Yale Child Study Center (TV), Department of Psychology (MDR, MMC), and Department of Neurobiology (MMC); and Department of Neurosurgery (RTC), Yale School of Medicine, Yale University, New Haven, Connecticut; Section on Functional Imaging Methods (ESF), National Institute of Mental Health, Bethesda, Maryland; Department of Psychology (MDR), University of Chicago, Chicago, Illinois; and Department of Psychiatry (MNS), College of Physicians and Surgeons, Columbia University, New York, New York.

Address correspondence to Evelyn M.R. Lake, Ph.D., Department of Radiology and Biomedical Imaging, Yale School of Medicine, Anlyan Center, 300 Cedar St. New Haven, CT 06519; E-mail: [evelyn.lake@yale.edu](mailto:evelyn.lake@yale.edu).

Received Jul 27, 2018; revised Feb 1, 2019; accepted Feb 2, 2019.

Received Jan 27, 2019; revised Feb 1, 2019; accepted Feb 21, 2019.  
Supplementary material cited in this article is available online at <https://doi.org/10.1016/j.biopsych.2019.02.019>.

## REFERENCES

- The authors report no biomedical financial interests or potential conflicts of interest.

## ARTICLE INFORMATION

From the Department of Radiology and Biomedical Imaging (EMRL, XS, DS, RTC), Interdepartmental Neuroscience Program (SMN, MMC, RTC), Yale Child Study Center (TV), Department of Psychology (MDR, MMC), and Department of Neurobiology (MMC); and Department of Neurosurgery (RTC), Yale School of Medicine, Yale University, New Haven, Connecticut; Section on Functional Imaging Methods (ESF), National Institute of Mental Health, Bethesda, Maryland; Department of Psychology (MDR), University of Chicago, Chicago, Illinois; and Department of Psychiatry (MNS), College of Physicians and Surgeons, Columbia University, New York, New York.

Address correspondence to Evelyn M.R. Lake, Ph.D., Department of Radiology and Biomedical Imaging, Yale School of Medicine, Anlyan Center, 300 Cedar St. New Haven, CT 06519; E-mail: [evelyn.lake@yale.edu](mailto:evelyn.lake@yale.edu).

Received Jul 27, 2018; revised Feb 1, 2019; accepted Feb 2, 2019.  
Supplementary material cited in this article is available online at <https://doi.org/10.1016/j.biopsych.2019.02.019>.

## REFERENCES

  - de Bildt A, Sytema S, Ketelaars C, Kraijer D, Mulder E, Volkmar F, et al. (2004): Interrelationship between autism diagnostic observation schedule-generic (ADOS-G), autism diagnostic interview-revised (ADI-R), and the diagnostic and statistical manual of mental disorders (DSM-IV-TR) classification in children and adolescents with mental retardation. *J Autism Dev Disord* 34:129–137.
  - Minschew NJ, Williams DL (2007): The new neurobiology of autism: Cortex, connectivity, and neuronal organization. *Arch Neurol* 64:945–950.
  - Baroni A, Castellanos FX (2015): Neuroanatomic and cognitive abnormalities in attention-deficit/hyperactivity disorder in the era of “high definition” neuroimaging. *Curr Opin Neurobiol* 30:1–8.
  - Boyle CA, Boulet S, Schieve LA, Cohen RA, Blumberg SJ, Yeargin-Allsopp M, et al. (2011): Trends in the prevalence of developmental disabilities in US children, 1997–2008. *Pediatrics* 127:1034–1042.
  - Erskine HE, Ferrari AJ, Nelson P, Polanczyk GV, Flaxman AD, Vos T, et al. (2013): Research review: Epidemiological modelling of attention-deficit/hyperactivity disorder and conduct disorder for the Global Burden of Disease Study 2010. *J Child Psychol Psychiatry* 54:1263–1274.
  - Reiersen AM, Constantino JN, Volk HE, Todd RD (2007): Autistic traits in a population-based ADHD twin sample. *J Child Psychol Psychiatry* 48:464–472.
  - Simonoff EMD, Pickles APD, Charman TPD, Chancier SPD, Loucas TPD, Baird GF (2008): Psychiatric disorders in children with autism spectrum disorders: Prevalence, comorbidity, and associated factors in a population-derived sample. *J Am Acad Child Adolesc Psychiatry* 47:921–929.
  - Sinzig J, Walter D, Doepfner M (2009): Attention deficit/hyperactivity disorder in children and adolescents with autism spectrum disorder: Symptom or syndrome? *J Atten Disord* 13:117–126.
  - Ray S, Miller M, Karalunas S, Robertson C, Grayson DS, Cary RP, et al. (2014): Structural and functional connectivity of human brain in autism spectrum disorders and attention-deficit/hyperactivity disorder: A rich club-organization study. *Hum Brain Mapp* 35:6032–6048.
  - Bethlehem RAI, Romero-Garcia R, Mak E, Bullmore ET, Baron-Cohen S (2017): Structural covariance networks in children with autism or ADHD. *Cereb Cortex* 27:4267–4276.
  - American Psychiatric Association (2013): Diagnostic and Statistical Manual of Mental Disorders, 5th ed. Arlington, VA: American Psychiatric Publishing.
  - Kern JK, Geier DA, Sykes LK, Geier MR, Seth RC (2015): Are ASD and ADHD a continuum? A comparison of pathophysiological similarities between the disorders. *J Atten Disord* 19:805–827.
  - Kern JK, Geier DA, King PG, Sykes LK, Mehta JA, Geier MR (2015): Shared brain connectivity issues, symptoms, and comorbidities in autism spectrum disorder, attention deficit/hyperactivity disorder, and Tourette syndrome. *Brain Connect* 5:321–335.
  - Dougherty CC, Evans DW, Myers SM, Moore GJ, Michael AM (2016): A comparison of structural brain imaging findings in autism spectrum disorder and attention-deficit hyperactivity disorder. *Neuropsychol Rev* 26:25–43.
  - Zhao H, Nyholt DR (2017): Gene-based analyses reveal novel genetic overlap and allelic heterogeneity across five major psychiatric disorders. *Hum Genet* 136:263–274.
  - Cross-Disorder Group of the Psychiatric Genomics Consortium (2013): Genetic relationship between five psychiatric disorders estimated from genome-wide SNPs. *Nat Genet* 45:984–994.
  - Rommelse NN, Franke B, Geurts HM, Hartman CA, Buitelaar JK (2010): Shared heritability of attention-deficit/hyperactivity disorder and autism spectrum disorder. *Eur Child Adolesc Psychiatry* 19:281–295.
  - Ogawa S, Lee TM, Kay AR, Tank DW (1990): Brain magnetic resonance imaging with contrast dependent on blood oxygenation. *Proc Natl Acad Sci U S A* 87:9868–9872.
  - Biswal B, Yetkin FZ, Haughton VM, Hyde JS (1995): Functional connectivity in the motor cortex of resting human brain using echo-planar MRI. *Magn Reson Med* 34:537–541.
  - Biswal BB, Mennes M, Zuo XN, Gohel S, Kelly C, Smith SM, et al. (2010): Toward discovery science of human brain function. *Proc Natl Acad Sci U S A* 107:4734–4739.
  - Finn ES, Shen X, Scheinost D, Rosenberg MD, Huang J, Cun MM, et al. (2015): Functional connectome fingerprinting: Identifying individuals using patterns of brain connectivity. *Nat Neurosci* 18:1664–1671.
  - Beaty RE, Kenett YN, Christensen AP, Rosenberg MD, Benedek M, Chen Q, et al. (2018): Robust prediction of individual creative ability from brain functional connectivity. *Proc Natl Acad Sci U S A* 115:1087–1092.
  - Rosenberg MD, Finn ES, Scheinost D, Papademetris X, Shen X, Constable RT, Chun MM (2016): A neuromarker of sustained attention from whole-brain functional connectivity. *Nat Neurosci* 19:165–167.
  - Rosenberg MD, Finn ES, Scheinost D, Constable RT, Chun MM (2017): Characterizing attention with predictive network models. *Trends Cogn Sci* 21:290–302.
  - Heare LJ, Mattingley JB, Cocchi L (2016): Functional brain networks related to individual differences in human intelligence at rest. *Sci Rep* 6:32328.
  - Uddin LQ, Supekar K, Menon V (2013): Reconceptualizing functional brain connectivity in autism from a developmental perspective. *Front Hum Neurosci* 7:458.
  - Redcay E, Moran JM, Mavros PL, Tager-Flusberg H, Gabrieli JD, Whitfield-Gabrieli S (2013): Intrinsic functional network organization in high-functioning adolescents with autism spectrum disorder. *Front Hum Neurosci* 7:573.
  - Ypma RJ, Moseley RL, Holt RJ, Rughoputh N, Floris DL, Chura LR, et al. (2016): Default mode hypoconnectivity underlies a sex-related autism spectrum. *Biol Psychiatry Cogn Neuroimaging* 1:364–371.
  - Cerlinani L, Mennes M, Thomas RM, Di Martino A, Thioux M, Keysers C (2015): Increased functional connectivity between subcortical and cortical resting-state networks in autism spectrum disorder. *JAMA Psychiatry* 72:767–777.
  - Wolfers T, Buitelaar JK, Beckmann CF, Franke B, Marquand AF (2015): From estimating activation locality to predicting disorder: A review of pattern recognition for neuroimaging-based psychiatric diagnostics. *Neurosci Biobehav Rev* 57:328–349.
  - Dos Santos Siqueira A, Biazoli CE Jr, Comfort WE, Rohde LA, Sato JR (2014): Abnormal functional resting-state networks in ADHD: Graph theory and pattern recognition analysis of fMRI data. *Biomed Res Int* 2014:380531.
  - Proal E, Olvera JG, White AS, Chalita PJ, Castellanos FX (2013): Neurobiology of autism and ADHD using neuroimaging techniques: Divergences and convergences [in Spanish]. *Rev Neurol* 57:S163–S175.
  - Chantiluke K, Christakou A, Murphy CM, Giampietro V, Daly EM, Ecker C, et al. (2014): Disorder-specific functional abnormalities during temporal discounting in youth with attention deficit hyperactivity disorder (ADHD), autism and comorbid ADHD and autism. *Psychiatry Res* 223:113–120.

34. Rane P, Cochran D, Hodge SM, Haselgrave C, Kennedy DN, Frazier JA (2015): Connectivity in autism: A review of MRI connectivity studies. *Harv Rev Psychiatry* 23:223–244.
35. Yarkoni T, Westfall J (2017): Choosing prediction over explanation in psychology: Lessons from machine learning. *Perspect Psychol Sci* 12:1100–1122.
36. Rausch A, Zhang W, Beckmann CF, Buitelaar JK, Groen WB, Haak KV (2018): Connectivity-based parcellation of the amygdala predicts social skills in adolescents with autism spectrum disorder. *J Autism Dev Disord* 48:572–582.
37. Bernhardt BC, Di Martino A, Valk SL, Wallace GL (2017): Neuroimaging-based phenotyping of the autism spectrum. *Curr Top Behav Neurosci* 30:341–355.
38. Hull JV, Jacokes ZJ, Torgerson CM, Irimia A, Van Horn JD (2017): Resting-state functional connectivity in autism spectrum disorder: A review. *Front Psychiatry* 7:205.
39. Nunes AS, Peatfield N, Vakorin V, Doesburg SM (2018): Idiosyncratic organization of cortical networks in autism spectrum disorder [published online ahead of print Jan 31]. *Neuroimage*.
40. Shen X, Finn ES, Scheinost D, Rosenberg MD, Chun MM, Papademetris X, et al. (2017): Using connectome-based predictive modeling to predict individual behavior from brain connectivity. *Nat Protoc* 12:506–518.
41. Shen X, Tokoglu F, Papademetris X, Constable RT (2013): Groupwise whole-brain parcellation from resting-state fMRI data for network node identification. *Neuroimage* 82:403–415.
42. Noble S, Scheinost D, Finn ES, Shen X, Papademetris X, McEwen SC, et al. (2017): Multisite reliability of MR-based functional connectivity. *Neuroimage* 146:959–970.
43. Di Martino A, Yan CG, Li Q, Denio E, Castellanos FX, Alaerts K, et al. (2014): The autism brain imaging data exchange: Towards a large-scale evaluation of the intrinsic brain architecture in autism. *Mol Psychiatry* 19:659–667.
44. Di Martino A, O'Connor D, Chen B, Alaerts K, Anderson JS, Assaf M, et al. (2017): Enhancing studies of the connectome in autism using the Autism Imaging Data Exchange II. *Sci Data* 4:170010.
45. ADHD-200 Consortium (2012): The ADHD-200 Consortium: A model to advance the translational potential of neuroimaging in clinical neuroscience. *Front Syst Neurosci* 2012 6:62.
46. Grzadzinski R, Dick C, Lord C, Bishop S (2016): Parent-reported and clinician-observed autism spectrum disorder (ASD) symptoms in children with attention deficit/hyperactivity disorder (ADHD): Implications for practice under DSM-5. *Mol Autism* 7:7.
47. Grzadzinski R, Di Martino A, Brady E, Mairena MA, O'Neale M, Petkova E, et al. (2011): Examining autistic traits in children with ADHD: Does the autism spectrum extend to ADHD? *J Autism Dev Disord* 41:1178–1191.
48. Insel T, Cuthbert B, Garvey M, Heinssen R, Pine DS, Quinn K, et al. (2010): Research domain criteria (RDoC): Toward a new classification framework for research on mental disorders. *Am J Psychiatry* 167:748–751.
49. Scheinost D, Papademetris X, Constable RT (2014): The impact of image smoothness on intrinsic functional connectivity and head motion confounds. *Neuroimage* 95:13–21.
50. Joshi A, Scheinost D, Okuda H, Belhachemi D, Murphy I, Staib LH, et al. (2011): Unified framework for development, deployment and robust testing of neuroimaging algorithms. *Neuroinformatics* 9:69–84.
51. Constantino JN, Davis SA, Todd RD, Schindler MK, Gross MM, Brophy SL, et al. (2003): Validation of a brief quantitative measure of autistic traits: Comparison of the social responsiveness scale with the Autism Diagnostic Interview-Revised. *J Autism Dev Disord* 33:427–433.
52. Lord C, Risi S, Lambrecht L, Cook EH Jr, Leventhal BL, DiLavore PC, et al. (2000): The autism diagnostic observation schedule-generic: A standard measure of social and communication deficits associated with the spectrum of autism. *J Autism Dev Disord* 30:205–223.
53. DuPaul GJ, Power TJ, Anastopoulos AD, Reid R (1998): *ADHD Rating Scale-IV: Checklists, Norms, and Clinical Interpretation*. New York, NY: Guilford Press, 25.
54. Rubinov M, Sporns O (2010): Complex network measures of brain connectivity: Uses and interpretations. *Neuroimage* 52:1059–1069.
55. Smith SM, Miller KL, Salimi-Khorshidi G, Webster M, Beckmann CF, Nichols TE, et al. (2011): Network modelling methods for fMRI. *Neuroimage* 54:875–891.
56. Wang Y, Kang J, Kemmer PB, Guo Y (2016): An efficient and reliable statistical method for estimating functional connectivity in large scale brain networks using partial correlation. *Front Neurosci* 10:123.
57. Greene AS, Gao S, Scheinost D, Constable RT (2018): Task-induced brain state manipulation improves prediction of individual traits. *Nat Commun* 9:2807.
58. Power JD, Barnes KA, Snyder AZ, Schlaggar BL, Petersen SE (2012): Spurious but systematic correlations in functional connectivity MRI networks arise from subject motion. *Neuroimage* 59:2142–2154.
59. Taurines R, Schwenck C, Westerwald E, Sachse M, Siniatchkin M, Freitag C (2012): ADHD and autism: Differential diagnosis or overlapping traits? A selective review. *Atten Defic Hyperact Disord* 4:115–139.
60. Craig F, Margari F, Legrottiglie AR, Palumbi R, de Giambattista C, Margari L (2016): A review of executive function deficits in autism spectrum disorder and attention-deficit/hyperactivity disorder. *Neuropsychiatr Dis Treat* 12:1191–1202.
61. Rubia K (2018): Cognitive neuroscience of attention deficit hyperactivity disorder (ADHD) and its clinical translation. *Front Hum Neurosci* 12:100.
62. Cortese S, Kelly C, Chabernaud C, Proal E, Di Martino A, Milham MP, et al. (2012): Towards systems neuroscience of ADHD: A meta-analysis of 55 fMRI studies. *Am J Psychiatry* 169:1038–1055.
63. Insel TR (2018): The NIMH research domain criteria (RDoC) project precision medicine for psychiatry. *Am J Psychiatry* 171:395–397.
64. Orban P, Dansereau C, Desbois L, Mongeau-Pérusse V, Giguère CÉ, Nguyen H, et al. (2018): Multisite generalizability of schizophrenia diagnosis classification based on functional brain connectivity. *Schizophr Res* 192:167–171.
65. Cremers HR, Wager TD, Yarkoni T (2017): The relation between statistical power and inference in fMRI. *PLoS One* 12:e0184923.
66. Noble S, Spann MN, Tokoglu F, Shen X, Constable RT, Scheinost D (2017): Influences of the test-retest reliability of functional connectivity MRI and its relationship with behavioral utility. *Cereb Cortex* 27:5415–5429.
67. Rosenberg MD, Hsu WT, Scheinost D, Todd Constable R, Chun MM (2018): Connectome-based models predict separable components of attention in novel individuals. *J Cogn Neurosci* 30:160–173.
68. Finn ES, Scheinost D, Finn DM, Shen X, Papademetris X, Constable RT (2017): Can brain state be manipulated to emphasize individual differences in functional connectivity. *Neuroimage* 160:140–151.
69. Vanderwal T, Kelly C, Eibott J, Mayes LC, Castellanos FX (2015): Inscapes: A movie paradigm to improve compliance in functional magnetic resonance imaging. *Neuroimage* 122:222–232.
70. Vanderwal T, Eibott J, Finn ES, Craddock RC, Turnbull A, Castellanos FX (2017): Individual difference in functional connectivity during naturalistic viewing conditions. *Neuroimage* 157:521–530.